

Article

Passively Q-Switched KTA Cascaded Raman Laser with 234 and 671 cm^{-1} Shifts

Zhi Xie ^{1,2}, Senhao Lou ², Yanmin Duan ², Zhihong Li ², Limin Chen ¹, Hongyan Wang ³, Yaoju Zhang ² and Haiyong Zhu ^{2,*} 

¹ College of Mechanical and Electronic Engineering, Fujian Agriculture and Forestry University, Fuzhou 350002, China; xzjau@126.com (Z.X.); chenlm1998@163.com (L.C.)

² Wenzhou Key Laboratory of Micro-Nano Optoelectronic Devices, Wenzhou University, Wenzhou 325035, China; 194511082199@stu.wzu.edu.cn (S.L.); ymduan@wzu.edu.cn (Y.D.); zhihong@wzu.edu.cn (Z.L.); zhangyj@wzu.edu.cn (Y.Z.)

³ Crystech Inc., Qingdao 266100, China; wanghongyan0401@hotmail.com

* Correspondence: hyzhu.opt@gmail.com

Abstract: A compact KTA cascaded Raman system driven by a passively Q-switched Nd:YAG/Cr⁴⁺:YAG laser at 1064 nm was demonstrated for the first time. The output spectra with different cavity lengths were measured. Two strong lines with similar intensity were achieved with a 9 cm length cavity. One is the first-Stokes at 1146.8 nm with a Raman shift of 671 cm^{-1} , and the other is the Stokes at 1178.2 nm with mixed Raman shifts of 234 cm^{-1} and 671 cm^{-1} . At the shorter cavity length of 5 cm, the output Stokes lines with high intensity were still at 1146.8 nm and 1178.2 nm, but the intensity of 1178.2 nm was higher than that of 1146.8 nm. The maximum average output power of 540 mW was obtained at the incident pump power of 10.5 W with the pulse repetition frequency of 14.5 kHz and the pulse width around 1.1 ns. This compact passively Q-switched KTA cascaded Raman laser can yield multi-Stokes waves, which enrich laser output spectra and hold potential applications for remote sensing and terahertz generation.

Keywords: raman laser; KTA crystal; passively Q-switch



Citation: Xie, Z.; Lou, S.; Duan, Y.; Li, Z.; Chen, L.; Wang, H.; Zhang, Y.; Zhu, H. Passively Q-Switched KTA Cascaded Raman Laser with 234 and 671 cm^{-1} Shifts. *Appl. Sci.* **2021**, *11*, 6895. <https://doi.org/10.3390/app11156895>

Academic Editor: Yung-Fu Chen

Received: 4 July 2021

Accepted: 20 July 2021

Published: 27 July 2021

Publisher's Note: MDPI stays neutral with regard to jurisdictional claims in published maps and institutional affiliations.



Copyright: © 2021 by the authors. Licensee MDPI, Basel, Switzerland. This article is an open access article distributed under the terms and conditions of the Creative Commons Attribution (CC BY) license (<https://creativecommons.org/licenses/by/4.0/>).

1. Introduction

Owing to its high optical damage threshold, broad transparency range, and high nonlinear coefficient together with the low ionic conductivity, potassium titanyl arsenate (KTA) is considered to be a promising crystal for nonlinear optics applications. For the past few decades, KTA has been extensively used to yield efficient eye-safe laser and mid-infrared laser via optical parametric oscillation [1–4]. Moreover, KTA has also attracted increasing attention due to its potential application for efficient stimulated Raman laser operation [5–7]. As an effective way to generate coherent light with new wavelengths, stimulated Raman scattering (SRS) has merits for preparing simple, compact, and robust laser sources [8–10]. Diverse crystals have been adopted for efficient Raman lasers, such as vanadates [11–13], tungstates [14–17], and molybdates [18]. Different from these commonly used Raman crystals, KTA and its isomorphs possess large Raman gain coefficient and small Raman shifts [19–22], such that it can generate a variety of high order Stokes lasers by cascade SRS.

In 1991, Watson first investigated the KTA Raman spectrum and identified a strong Raman shift of 234 cm^{-1} [5]. Based on the intracavity pumped KTA using a Nd:YAG/KTA Raman configuration, Liu et al. studied the first and second-Stokes lasers at 1091 nm and 1120 nm, respectively [6,21]. Lan et al. also surveyed the Raman laser of 1091 nm using a passively Q-switched Nd:YAG/KTA configuration, and a 250 mW power was realized with the conversion efficiency of 3.3% [22]. Based on the Nd:YAP/KTA configuration, Huang et al. reported a simultaneous dual-wavelength eye-safe Raman laser [23]. Liu et al.

reported the second harmonic generation (SHG) laser converted from the first-Stokes in KTA Raman with the shift of 671 cm^{-1} [24]. Our group also studied the multi-Stokes waves from cascade Raman conversion based on a KTA crystal [25]. From the main Raman shifts of 671 cm^{-1} and 234 cm^{-1} in the KTA crystal, the gains of high order Stokes waves can enrich laser spectral lines which cannot be directly produced from the laser crystal doped with rare earth ions [26]. In addition, via the processes of the SHG and sum frequency generation (SFG), the Stokes waves can produce visible light which has important applications in remote sensing, visual displays, and medical treatments [27,28]. The simultaneous multi-order Stokes waves output has also been reported to be a prospective pumping source for the terahertz (THz) wave generation employing the nonlinear optics method [29].

A solid-state laser based on Cr^{4+} :YAG passively Q-switching has the advantages of compactness and low cost for high pulse repetition frequency pulse laser operation [30–32]. Therefore, a passively Q-switched cascaded Raman laser could be a compact and efficient laser system for Stokes laser output. In this work, for the first time, multi-Stokes waves from passively Q-switched KTA cascaded Raman lasers were studied. A Nd:YAG/ Cr^{4+} :YAG composite crystal was used as the saturable absorber. Under a pumping power of 10.5 W and pulse repetition frequency of 14.5 kHz (for the setup with a 5 cm length cavity) the largest average output power of 540 mW was realized with a pulse width of about 1.1 ns. The measured spectra show various Stokes lines in the range of 1050–1200 nm, which were converted via the Raman shifts of 234 cm^{-1} and 671 cm^{-1} , and two strong lines were located at 1146.8 nm and 1178.2 nm.

2. Experimental Setup

KTA is an anisotropic optical crystal of the orthotropic crystal system. According to the polarization-dependent spontaneous Raman scattering spectra of x-axis cut KTA crystals, strong Raman scattering with two main Raman shifts at 234 cm^{-1} and 671 cm^{-1} can be realized from the A1 (ZZ) geometry. Therefore, an x-axis cut KTA crystal of $4 \times 4 \times 20\text{ mm}^3$ dimension was employed as the Raman medium to satisfy the X(ZZ)X Raman configuration, according to Porto notations. The KTA crystal was placed in a compact plane-concave cavity and driven by the passively Q-switched Nd:YAG laser at 1064 nm. Figure 1 shows the diagrammatic sketch of the passively Q-switched KTA cascaded Raman laser experimental setup. The Nd:YAG crystal composited with Cr^{4+} :YAG crystal in order to make the system more compact and easy to dissipate heat, and these two crystals were used to serve as the laser gain medium and the saturable absorber for passively Q-switching, respectively. The Nd:YAG crystal with the size of $3 \times 3 \times 7\text{ mm}^3$ is 1.0 at.% doped, and the Cr^{4+} :YAG crystal with size of $3 \times 3 \times 3\text{ mm}^3$ has an initial transmission of about 85%. While the optics was closed set with each other, the total cavity length was about 50 mm.

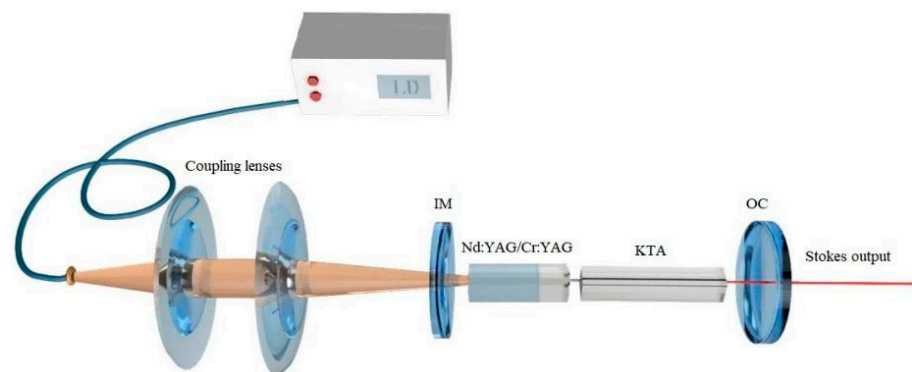


Figure 1. Experimental setup of the passively Q-switched KTA cascaded Raman laser.

The pumping source is a fiber-coupled laser diode array operating at 808 nm, which has a fiber core diameter of $200\text{ }\mu\text{m}$ and a numerical aperture of 0.22. The pump beam was re-imaged by two 808 nm anti-reflection (AR) coated achromatic lenses with focal lengths

of 50 and 80 mm, obtaining a beam waist of about 320 μm in the Nd:YAG crystal. Both the Nd:YAG/Cr⁴⁺:YAG composite crystal and the KTA crystal were wrapped with indium foil and mounted in a thermoelectric-cooled copper block with the temperature kept at about 20 °C throughout the experiments. Both end-faces of the composite crystal and the KTA crystal were AR coated for the fundamental and Stokes wavelengths from 1000 to 1200 nm, and the pump light incident face of the Nd:YAG crystal was AR coated at 808 nm.

3. Results and Discussion

Table 1 lists Stokes wavelengths with contributed Raman shifts. It can be seen that there are many Stokes wavelengths ranging from 1050 to 1200 nm, which were yielded via two Raman shifts of 234 cm^{-1} and 671 cm^{-1} . The fundamental and Raman laser oscillation shared the identical plane-concave linear cavity constituted by the input mirror (IM) and the output coupler (OC) mirror. The IM was high-transmission (HT, $T > 98\%$) coated at 808 nm and high-reflection (HR, $R > 99.9\%$) coated from 1000 to 1200 nm. The OC mirror with a radius curvature of 100 mm was HR coated for the range of 1050–1130 nm. The transmittance curve of the output coupler is displayed in Figure 2. With the wavelength larger than 1130 nm, the transmittance increased, reaching 1.5% at 1147 nm and 67% at 1182 nm.

Table 1. Stokes wavelengths with contributed Raman shifts.

Wavelength (nm)	Contributed Raman Shifts $\omega_{R1} = 234 \text{ cm}^{-1}$, $\omega_{R2} = 671 \text{ cm}^{-1}$
1092.0	ω_{R1}
1120.7	$2\omega_{R1}$
1146.8	ω_{R2}
1150.4	$3\omega_{R1}$
1178.2	$\omega_{R2} + \omega_{R1}$
1182.4	$4\omega_{R1}$

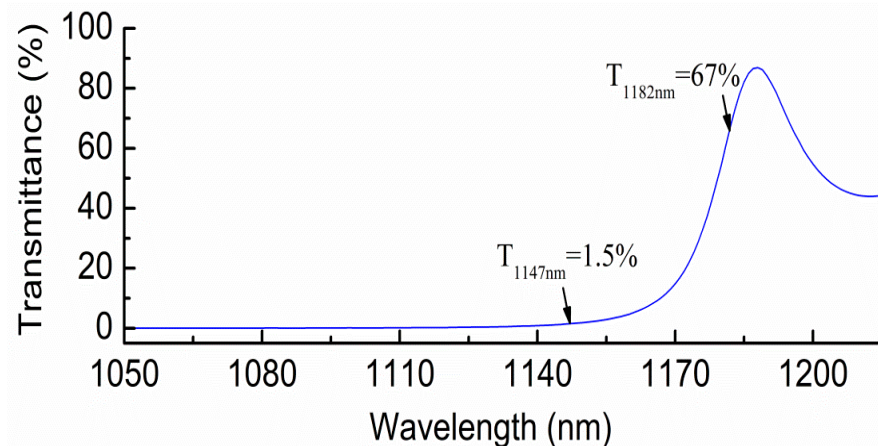


Figure 2. Transmittance curve of the OC mirror for different wavelengths.

The KTA Raman laser output characteristics were optimized by adjusting the pump power and cavity length. The maximum power of the output was achieved under a pump power of 10.5 W. The data of the output power were detected using the thermal sensor power meter (PM310D, Thorlabs INC). Figure 3 exhibits the average output power for two cavity lengths of 5 cm and 9 cm, with respect to the incident pump power. It is shown that the Raman threshold for a 5 cm length cavity was around 3.4 W, and for a 9 cm length cavity it was around 4.9 W. For the two cavity length setups, the average output powers both raised with the increase of incident pump power, provided with the slope efficiency of 7.6% for the 5 cm length cavity and 8.0% for the 9 cm length cavity. A lower Raman threshold for 5 cm length cavity benefited from its low cavity loss with the short and compact laser

cavity, and the 5 cm length cavity is more suitable for high output power than the 9 cm length cavity with an increase of pump power. Under an incident pump power of 10.5 W, the obtained maximum output powers were 530 mW for the setup with 5 cm length cavity, and 320 mW for the setup with 9 cm length cavity. The power instability at the maximum output for these two length cavities were better than 5%.

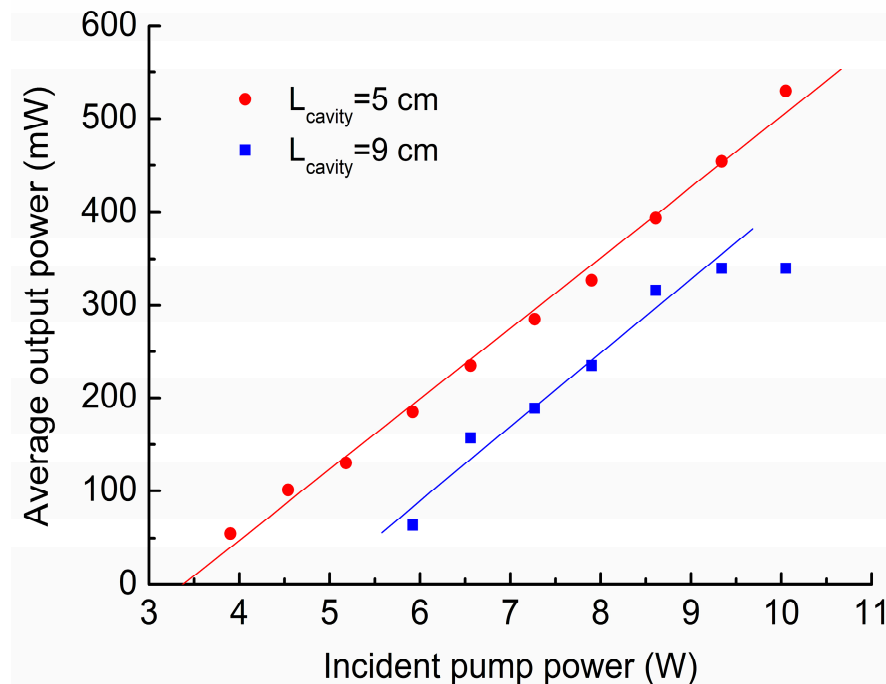


Figure 3. Average output power versus incident pump power of the Raman lasers with the cavity lengths of 5 cm and 9 cm.

Figure 4 displays the laser spectra with the 5 cm and 9 cm cavity lengths, respectively. The data were measured at the pump power of 10.5 W using a grating monochromator (Omni- λ 500 model, ZOLIX, Beijing, China). According to the wavelengths and Raman shifts shown in Table 1, the spectra lines can be identified. For the setup with the 9 cm length cavity, its spectrum contains two strong lines with similar intensity, which are the first-Stokes at 1146.8 nm with the Raman shift of 671 cm^{-1} , and the Stokes at 1178.2 nm with mixed Raman shifts of 234 cm^{-1} and 671 cm^{-1} . Four low intensity lines were also detected. They are the fundamental wave at 1064 nm, the first, second and third-Stokes at 1092.0, 1120.7, and 1150.4 nm, respectively, with a Raman shift of 234 cm^{-1} . For the setup with 5 cm length cavity, due to the lower loss caused by the shorter cavity length, the low order Stokes were converted to higher order Stokes. The first-Stokes at 1092.0 nm and the second-Stokes at 1120.7 nm became negligible, while the intensity of 1178.2 nm was significantly enhanced, and more obvious third-Stokes (1150.4 nm) and fourth-Stokes (1182.4 nm) waves with Raman shift of 234 cm^{-1} were also observed. However, the output was still dominated by the Stokes waves at 1178.2 nm and 1146.8 nm. Therefore, different cavity lengths also resulted in the difference of output spectra, which might be mainly attributed to the intensity distribution changing in the cavity.

The pulse width and pulse repetition frequency with different incident pump powers were obtained using the free-space InGaAs photodetector and exhibited on the 500 MHz oscilloscope (DPO3052B model). In view of the fact that the measured multi-Stokes wavelengths were very close to each other, and they cannot be segregated in our investigation, only the whole temporal pulse profiles of the Stokes waves were provided. As shown in Figure 5, with the incident pump power changed from 3.9 W to 10 W, the pulse repetition frequency went up from 2.9 kHz to 14.5 kHz, and the pulse energy rose from 21 μJ to 36 μJ except for a small decline when the incident pump changed from 4.5 W to 5.2 W. The pulse

repetition frequency was not as stable when the instability reached about 25%, which might be caused by the competition of multi-Stokes generation.

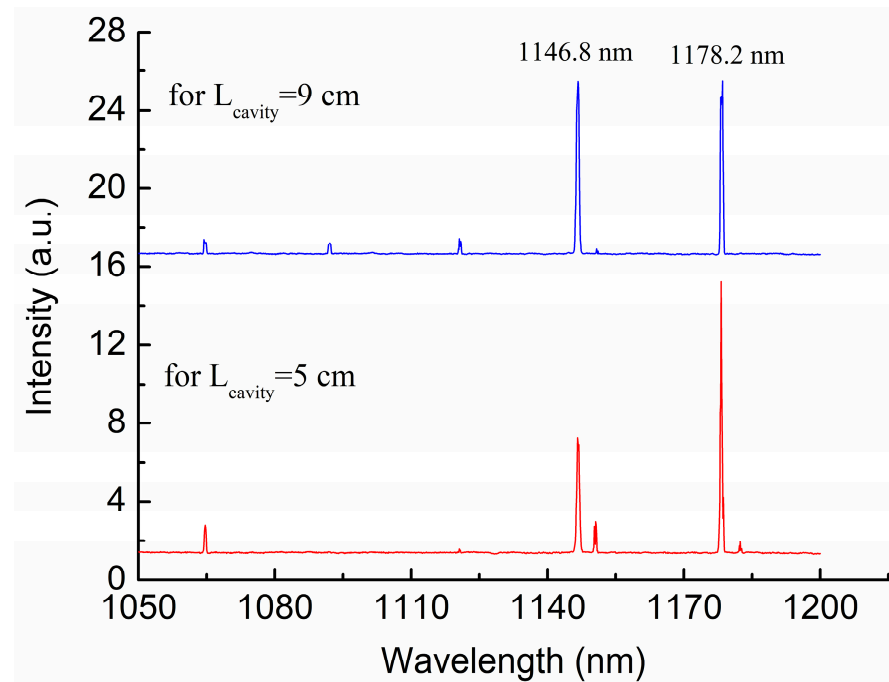


Figure 4. Raman laser spectra measured under the incident pump power of 10.5 W with the cavity lengths of 5 cm and 9 cm.

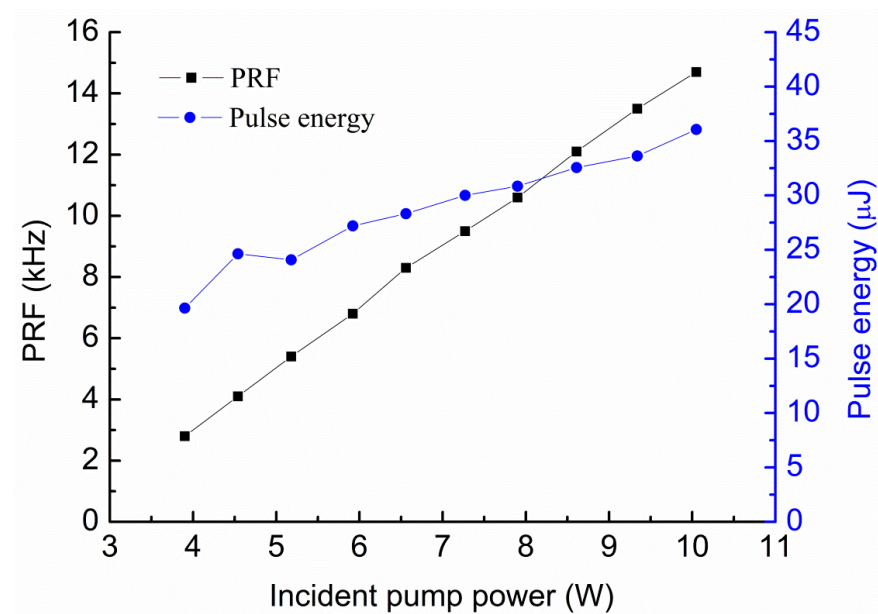


Figure 5. Pulse repetition frequency (PRF) and pulse energy versus incident pump power.

The measured pulse trains and temporal pulse profiles at the incident pump power of 10.5 W are displayed in Figure 6. The pulse width was around 1.1 ns, and the pulse repetition frequency was 14.5 kHz. A smaller value of pulse width than 1.1 ns might be more accurate, since the critical time resolution of the used 500 MHz oscilloscope was limited. We also measured the pulse width of weak leaked fundamental laser at 1064 nm, and the obtained value was around 11 ns. Therefore, significant pulse shortening was

detected for this KTA Raman laser which is similar to the fact that achieved in SrMoO₄ Raman laser [33].

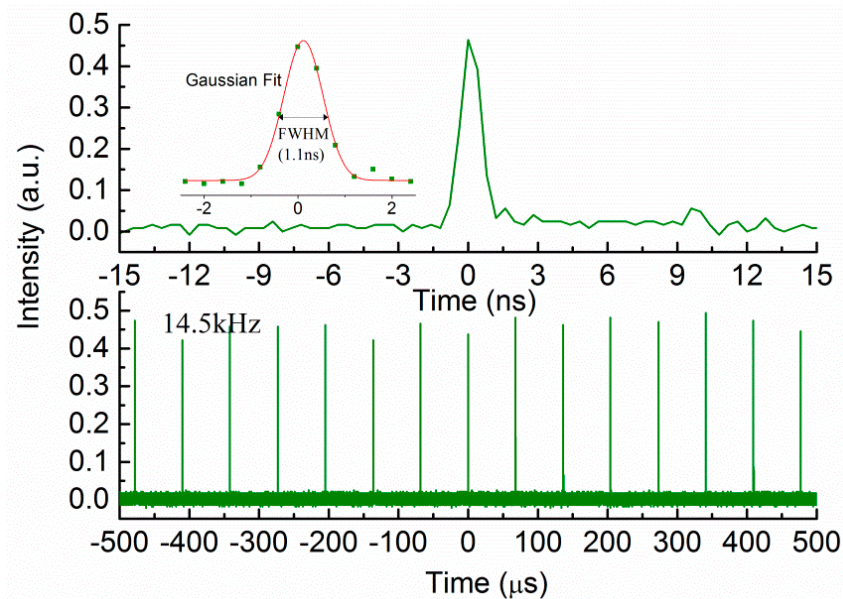


Figure 6. Temporal pulse profiles and pulse trains under the incident pump power of 10.5 W.

The spectra of the weak visible light accompanying with the Stokes wave output have been measured using a fiber optic spectrometer (AvaSpec-3648 model). The measured spectra are shown in Figure 7. It can be seen that the main lines are located at 573.4 nm and 574.3 nm, and the former can be assigned to the SHG of 1146.8 nm, while the latter is from the SFG of 1146.8 nm and 1150.4 nm with the phase matching angle θ of 82~83° in the x-z plane of KTA crystal. These weak visible lights possessed an output power of about a dozen milliwatts, which should be ascribed to the fact that the phase matching directions of SHG and SFG for the Stokes waves in the cavity were close to the x-axis. To our surprise, the SFG light (567 nm) of 1120.7 nm and 1146.8 nm was not observed. As known from the calculation, the SFG matching angle between these two wavelengths is closer to the x-axis of the KTA crystal compared with those for 573.4 nm and 574.3 nm light generation. The absence of 567 nm SFG light could be attributed to the light conversion from 1120.7 nm to 1150.4 nm due to high reflection of the resonant cavity for 1120.7 nm. Therefore, the 567 nm SFG light was negligible in contrast to the lines of 573.4 and 574.3 nm.

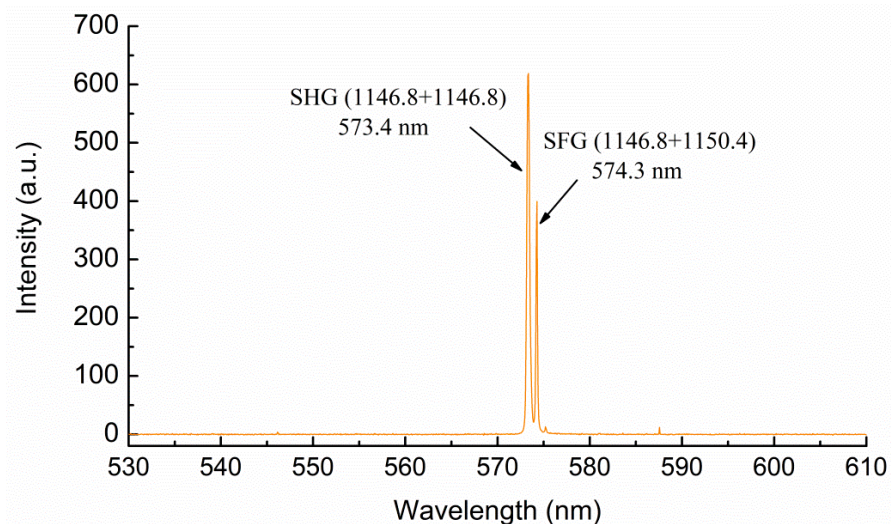


Figure 7. Spectra of weak visible light irradiated from the KTA crystal.

4. Conclusions

In summary, a compact passively Q-switched KTA cascaded Raman laser was demonstrated for the first time. A composite crystal of Nd:YAG/Cr⁴⁺:YAG was used for passively Q-switched fundamental laser generation at 1064 nm. The obtained multi-Stokes laser wavelengths range from 1090 to 1200 nm. The output spectra with two different cavity lengths were measured. Two strong lines with similar intensity were achieved with a 9 cm length cavity. One is the first-Stokes at 1146.8 nm with Raman shift of 671 cm⁻¹, and the other is the Stokes at 1178.2 nm with mixed Raman shifts of 234 cm⁻¹ and 671 cm⁻¹. For the setup with a shorter length cavity of 5 cm, some conversions from low order Stokes to higher order Stokes occurred due to the lower loss caused by the shorter cavity length, and the output Stokes waves with high intensity were still at 1146.8 nm and 1178.2 nm. However, the intensity of 1178.2 nm was obviously higher than that of 1146.8 nm. Under an incident pump power of 10.5 W, the measured maximum average output power was 540 mW. The measured pulse width was around 1.1 ns, and the pulse repetition frequency was 14.5 kHz. This compact passively Q-switched KTA cascaded Raman laser can yield multi-Stokes waves, which enrich laser output spectra lines and hold potential applications for remote sensing and terahertz generation.

Author Contributions: Conceptualization, Z.X., Y.D., and H.Z.; validation, Z.X. and S.L.; formal analysis, Z.X., S.L., Z.L., Y.Z., and H.Z.; resources, H.W.; writing—original draft preparation, Z.X. and S.L.; writing—review and editing, Y.D., Z.L., L.C., Y.Z. and H.Z.; supervision, Y.D. and H.Z. All authors have read and agreed to the published version of the manuscript.

Funding: This research was funded by the Zhejiang Provincial Natural Science Foundation of China under (Grant No. LY19F050012), the National Natural Science Foundation of China under (Grant No. 62075167 and No. 61905180), the public welfare projects of Wenzhou city under (Grant No. G2020013 and No. S20180015), and the Natural Science Foundation of Fujian Province (Grant No. 2019J01403).

Institutional Review Board Statement: Not applicable.

Informed Consent Statement: Not applicable.

Data Availability Statement: All of the data reported in the paper are presented in the main text. Any other data will be provided on request.

Conflicts of Interest: The authors declare no conflict of interest.

References

1. Powers, P.E.; Ramakrishna, S.; Tang, C.L.; Cheng, L.K. Optical parametric oscillation with KTiOAsO₄. *Opt. Lett.* **1993**, *18*, 1171–1173. [[CrossRef](#)]
2. Zhu, H.Y.; Guo, J.H.; Duan, Y.M.; Zhang, J.; Zhang, Y.C.; Xu, C.W.; Wang, H.Y.; Fan, D.Y. Efficient 1.7 μm light source based on KTA-OPO derived by Nd:YVO₄ self-Raman laser. *Opt. Lett.* **2018**, *43*, 345–348. [[CrossRef](#)]
3. Zhong, K.; Yao, J.Q.; Xu, D.G.; Wang, J.L.; Li, J.S.; Wang, P. High-pulse-energy high-efficiency midinfrared generation based on KTA optical parametric oscillator. *Appl. Phys. B* **2010**, *100*, 749–753. [[CrossRef](#)]
4. Duan, Y.M.; Zhu, H.Y.; Xu, C.W.; Ruan, X.K.; Cui, G.H.; Zhang, Y.J.; Tang, D.Y.; Fan, D.Y. Compact self-cascaded KTA-OPO for 2.6 μm laser generation. *Opt. Express* **2016**, *24*, 26529–26535. [[CrossRef](#)] [[PubMed](#)]
5. Watson, G.H. Polarized Raman spectra of KTiOAsO₄ and isomorphous nonlinear-optical crystals. *J. Raman Spectrosc.* **1991**, *22*, 705–713. [[CrossRef](#)]
6. Liu, Z.; Wang, Q.; Zhang, X.; Zhang, S.; Chang, J.; Cong, Z.; Sun, W.; Jin, G.; Tao, X.; Sun, Y.; et al. A diode side-pumped KTiOAsO₄ Raman laser. *Opt. Express* **2009**, *17*, 6968–6974. [[CrossRef](#)] [[PubMed](#)]
7. Guo, J.H.; Duan, Y.M.; Wang, H.Y.; Zhu, H.Y.; Wei, P.F.; Zhang, J.; Zhao, L.M.; Tang, D.Y. Efficient Nd:YAG\KTiOAsO₄ cascaded Raman laser emitting around 1.2 μm. *Opt. Mater.* **2017**, *71*, 66–69. [[CrossRef](#)]
8. Piper, J.A.; Pask, H.M. Crystalline Raman Lasers. *IEEE J. Sel. Top. Quantum Electron.* **2007**, *13*, 692–704. [[CrossRef](#)]
9. Sheng, Q.; Ma, H.; Li, R.; Wang, M.; Shi, W.; Yao, J. Recent progress on narrow-linewidth crystalline bulk Raman lasers. *Results Phys.* **2020**, *17*, 103073. [[CrossRef](#)]
10. Gong, X.H.; Zhu, H.Y.; Chen, Y.J.; Huang, J.H.; Lin, Y.F.; Luo, Z.D.; Huang, Y.D. Nd³⁺ Cluster Adjustment in Nd³⁺:CaNb₂O₆ by Codoping La³⁺ Buffers for Improvement of Fundamental and Self-Stimulated Raman Scattering Laser Operation: A Study Case from the Perspective of Defect Chemistry. *Cryst. Growth Des.* **2019**, *19*, 6963–6971. [[CrossRef](#)]
11. Zhang, L.; Duan, Y.M.; Mao, X.H.; Li, Z.H.; Chen, Y.X.; Zhang, Y.J.; Zhu, H.Y. Passively Q-switched YVO₄ Raman operation with 816 and 890 cm⁻¹ shifts by respective Raman configurations. *Opt. Mater. Express* **2021**, *11*, 1815–1823. [[CrossRef](#)]

12. Liu, Y.C.; Chen, C.M.; Hsiao, J.Q.; Pan, Y.Y.; Tsou, C.H.; Liang, H.C.; Chen, Y.F. Compact efficient high-power triple-color Nd:YVO₄ yellow-lime-green self-Raman lasers. *Opt. Lett.* **2020**, *45*, 1144–1147. [[CrossRef](#)] [[PubMed](#)]
13. Sun, Y.L.; Duan, Y.M.; Zhang, L.; Yang, Z.Y.; Chen, X.; Huang, X.H.; Zhu, H.Y. Efficient actively Q-switched Nd:YAP/YVO₄ Raman laser operation at 1195nm. *J. Russ. Laser Res.* **2020**, *41*, 373–377. [[CrossRef](#)]
14. Liu, Z.J.; Rao, H.; Cong, Z.H.; Xue, F.; Gao, X.B.; Wang, S.; Tan, W.; Guan, C.; Zhang, X.Y. Single-frequency BaWO₄ Raman MOPA at 1178 nm with 100-ns pulse pump. *Crystals* **2019**, *9*, 185. [[CrossRef](#)]
15. Duan, Y.M.; Zhu, H.Y.; Zhang, G.; Huang, C.H.; Wei, Y.; Tu, C.Y.; Zhu, Z.J.; Yang, F.G.; You, Z.Y. Efficient 559.6 nm light produced by sum-frequency generation of diode-end-pumped Nd:YAG/SrWO₄ Raman laser. *Laser Phys. Lett.* **2010**, *7*, 491–494. [[CrossRef](#)]
16. Chen, Y.F.; Huang, H.Y.; Lee, C.C.; Hsiao, J.Q.; Tsou, C.H.; Liang, H.C. High-power diode-pumped Nd:GdVO₄/KGW Raman laser at 578 nm. *Opt. Lett.* **2020**, *45*, 5562–5565. [[CrossRef](#)]
17. Sheng, Q.; Lee, A.; Spence, D.; Pask, H. Wavelength tuning and power enhancement of an intracavity Nd:GdVO₄-BaWO₄ Raman laser using an etalon. *Opt. Express* **2018**, *26*, 32145–32155. [[CrossRef](#)] [[PubMed](#)]
18. Yu, H.H.; Li, Z.; Lee, A.J.; Li, J.; Zhang, H.J.; Wang, J.Y.; Pask, H.M.; Piper, J.A.; Jiang, M.H. A continuous wave SrMoO₄ Raman laser. *Opt. Lett.* **2011**, *36*, 579–581. [[CrossRef](#)] [[PubMed](#)]
19. Tu, C.S.; Guo, A.R.; Tao, R.W.; Katiyar, R.S.; Guo, R.Y.; Bhalla, A.S. Temperature dependent Raman scattering in KTiOPO₄ and KTiOAsO₄ single crystals. *J. Appl. Phys.* **1996**, *79*, 3235–3240. [[CrossRef](#)]
20. Duan, Y.M.; Zhu, H.Y.; Zhang, Y.J.; Zhang, G.; Zhang, J.; Tang, D.Y.; Kaminskii, A.A. RbTiOPO₄ cascaded Raman operation with multiple Raman frequency shifts derived by Q-switched Nd:YAlO₃ laser. *Sci. Rep.* **2016**, *6*, 33852. [[CrossRef](#)] [[PubMed](#)]
21. Liu, Z.J.; Wang, Q.P.; Zhang, X.Y.; Zhang, S.S.; Chang, J.; Wang, H.; Fan, S.Z.; Sun, W.J.; Tao, X.T.; Zhang, S.J.; et al. 1120 nm second-Stokes generation in KTiOAsO₄. *Laser Phys. Lett.* **2008**, *6*, 121–124. [[CrossRef](#)]
22. Lan, W.X.; Wang, Q.P.; Liu, Z.J.; Zhang, X.Y.; Bai, F.; Shen, H.B.; Gao, L. A diode end-pumped passively Q-switched Nd:YAG/KTA Raman laser. *Optik* **2013**, *124*, 6866–6868. [[CrossRef](#)]
23. Huang, Y.J.; Chen, Y.F.; Chen, W.D.; Zhang, G. Dual-wavelength eye-safe Nd:YAP Raman laser. *Opt. Lett.* **2015**, *40*, 3560–3563. [[CrossRef](#)]
24. Liu, Z.; Wang, Q.; Zhang, X.; Zhang, S.; Chang, J.; Fan, S.; Sun, W.; Jin, G.; Tao, X.; Sun, Y.; et al. Self-frequency-doubled KTiOAsO₄ Raman laser emitting at 573 nm. *Opt. Lett.* **2009**, *34*, 2183–2185. [[CrossRef](#)] [[PubMed](#)]
25. Zhu, H.Y.; Shao, Z.H.; Wang, H.Y.; Duan, Y.M.; Zhang, J.; Tang, D.Y.; Kaminskii, A.A. Multi-order Stokes output based on intra-cavity KTiOAsO₄ Raman crystal. *Opt. Express* **2014**, *22*, 19662–19667. [[CrossRef](#)]
26. Duan, Y.; Zhu, H.; Wang, H.; Zhang, Y.; Chen, Z. Comparison of 1.15 μm Nd:YAG/KTA Raman lasers with 234 and 671 cm⁻¹ shifts. *Opt. Express* **2016**, *24*, 5565–5571. [[CrossRef](#)] [[PubMed](#)]
27. Pask, H.M.; Dekker, P.; Mildren, R.P.; Spence, D.J.; Piper, J.A. Wavelength-versatile visible and UV sources based on crystalline Raman lasers. *Prog. Quantum Electron.* **2008**, *32*, 121–158. [[CrossRef](#)]
28. Runcorn, T.H.; Gorlitz, F.G.; Murray, R.T.; Kelleher, E.J.R. Visible Raman-Shifted Fiber Lasers for Biophotonic Applications. *IEEE J. Sel. Topics Quantum Electron.* **2018**, *24*, 2770101. [[CrossRef](#)]
29. Chang, Y.T.; Huang, Y.P.; Su, K.W.; Chen, Y.F. Diode-pumped multi-frequency Q-switched laser with intracavity cascade Raman emission. *Opt. Express* **2008**, *16*, 8286–8291. [[CrossRef](#)]
30. Ye, P.P.; Zhu, S.Q.; Li, Z.; Yin, H.; Zhang, P.X.; Fu, S.H.; Chen, Z.Q. Passively Q-switched dual-wavelength green laser with an Yb:YAG/Cr⁴⁺:YAG/YAG composite crystal. *Opt. Express* **2017**, *25*, 5179–5185. [[CrossRef](#)]
31. Duan, Y.; Zhang, J.; Zhu, H.; Zhang, Y.; Xu, C.; Wang, H.; Fan, D. Compact passively Q-switched RbTiOPO₄ cascaded Raman operation. *Opt. Lett.* **2018**, *43*, 4550–4553. [[CrossRef](#)] [[PubMed](#)]
32. Dascalu, T.; Croitoru, G.; Grigore, O.; Pavel, N. High-peak-power passively Q-switched Nd:YAG/Cr⁴⁺:YAG composite laser with multiple-beam output. *Photon. Res.* **2016**, *4*, 267–271. [[CrossRef](#)]
33. Frank, M.; Smetanin, S.N.; Jelínek, M.; Vyhlídal, D.; Kopalkin, A.A.; Shukshin, V.E.; Ivleva, L.I.; Zverev, P.G.; Kubeček, V. Synchronously-pumped all-solid-state SrMoO₄ Raman laser generating at combined vibrational Raman modes with 26-fold pulse shortening down to 1.4 ps at 1220 nm. *Opt. Laser Technol.* **2019**, *111*, 129–133. [[CrossRef](#)]